

Comprehensive 3D Multiphysics Model on Electrochemical Recovery of O₂ from Metabolic CO₂ at the International Space Station (ISS)

Jesus A. Dominguez¹,

Insight Global/Jacobs Space Exploration Group (JSEG), Huntsville, AL, 35806

Brittany Brown², Lorlyn Reidy³, Kagen Crawford⁴, Kaitlin Oliver-Butler⁵, Cara Black⁶

NASA Marshall Space Flight Center, Huntsville, Alabama, 35811

Shannon McCall⁷

Qualis Corporation /Jacobs Space Exploration Group (JSEG), Huntsville, AL, 35806

Brian Dennis⁸ and Wilaiwan Chanmanee⁹

University of Texas at Arlington, Arlington, Texas, 76019

Kenneth A Burke¹⁰,

NASA Glenn Research Center, Cleveland, Ohio 44135

The International Space Station (ISS) is presently equipped with an elaborate, heavy, and high-power consuming system that recovers approximately 50% of O₂ from metabolic CO₂ as part of the atmospheric revitalization (AR) at the ISS habitat. Future long duration missions will require a more sustainable and efficient system capable of yielding a minimum of 75% O₂ recovery to reach the self-sufficiency required for long-duration space missions beyond Earth's low orbit. A Macrofluidic Electrochemical Reactor (MFECR) technology development effort is currently underway at NASA Marshall Space Flight Center (MSFC) to not only increase significantly current O₂ recovery efficiency, improving self-sufficiency on AR at the ISS habitat and future long-duration missions, but also reduce system complexity. The authors have developed and deployed a comprehensive 3D multiphysics model that thoroughly replicates the actual configuration and fluid/material domains of the MFECR. The coupled physics in this multiphysics model include multicomponent-multiphase electrochemical-driven reactions, non-ideal mass transport mechanism, free and porous flow, heat transfer, CO₂ solubility on alkaline electrolyte, water condensation on porous medium, and DC electrical current generation along with Joule heating effect. This model is aimed to conduct qualitative benchmark on three different MFECR layouts, one without serpentine paths (plain) and two with serpentines leading to four and twelve paths respectively. Once experimental data is generated via a test matrix of 200 tests, the model will be validated to conduct MFECR's process optimization and revalidate the qualitative benchmark on three different MFECR's layouts.

¹ ECLSS Principal Investigator, MSFC ECLSS Development Branch, Mail Stop: ES62, MSFC, AL 35812.

² ECLSS Engineer, MSFC ECLSS Development Branch, Mail Stop: ES62, MSFC, AL 35812.

³ Ionic Liquids Chemist, MSFC Materials Science & Metallurgy Branch, Mail Stop: EM22, MSFC, AL 35812.

⁴ Chemical Engineer, MSFC ECLSS Development Branch, Mail Stop: ES62, MSFC, AL 35812.

⁵ Aerospace Engineer, MSFC ECLSS Development Branch, Mail Stop: ES62, MSFC, AL 35812.

⁶ Acting Deputy Branch Chief, MSFC ECLSS Development Branch, Mail Stop: ES62, MSFC, AL 35812.

⁷ Senior Mechanical Engineer, MSFC ECLSS Development Branch, Mail Stop: ES62, MSFC, AL 35812.

⁸ Associate Professor, Dept. of Mechanical & Aerospace Engineering, 701 S. Nedderman Dr. Arlington, TX 76019.

⁹ Research Associate, Dept. of Mechanical & Aerospace Engineering, 701 S. Nedderman Dr. Arlington, TX 76019.

¹⁰ Electrical Engineer, Photovoltaic & Electrochemical Systems Branch, Mail Stop: LEX0, 21000 Brookpark Rd. Cleveland, OH 44135.

Nomenclature

<i>AR</i>	= <i>atmospheric revitalization</i>
<i>CDRS</i>	= <i>carbon dioxide reduction system</i>
<i>CL</i>	= <i>catalysis layer</i>
<i>EC</i>	= <i>electrochemical</i>
CO_2	= carbon dioxide
C_2H_4	= ethylene
<i>EDU</i>	= engineering design unit
<i>ECLSS</i>	= environmental control and life support system
<i>GC</i>	= gas chromatograph
<i>GDL</i>	= gas diffusion layer
<i>GDE</i>	= gas diffusion electrode
<i>CL</i>	= catalysis layer
KOH	= potassium hydroxide
<i>MFECR</i>	= macrofluidic electrochemical reactor
<i>MPL</i>	= macropore layer
<i>MSFC</i>	= Marshall Space Flight Center
<i>NASA</i>	= National Aeronautics and Space Administration
<i>OGA</i>	= oxygen generation assembly
O_2	= oxygen
OH^-	= hydroxide ion
<i>PDE</i>	= partial differential equations
<i>Pt</i>	= Platinum
<i>PTFE</i>	= poly-tetra-fluoro-ethylene
H_2	= hydrogen
<i>ISS</i>	= international space station
<i>UTA</i>	= university of Texas at Arlington

I. Introduction

Removal of metabolic carbon dioxide (CO_2) is crucial in Atmospheric Revitalization (AR) at the ISS and any other livable space habitat to maintain a safe, breathable atmosphere inside the habitat. The critical objective for the AR system is to 'close the loop', that is, to capture gaseous human metabolic products, specifically water (H_2O) vapor and CO_2 , for maximum O_2 recovery and to make other useful resources from these products. The AR subsystem also removes trace chemical contaminants from the habitat atmosphere to preserve habitat atmospheric quality, provide O_2 , and utilize instrumentation to monitor cabin atmospheric quality. Long-duration crewed space exploration missions will require critical advancements in AR process technologies to increase efficiency on O_2 recovery, reduce power and mass consumption, and increase reliability compared to prior AR processes used for shorter duration missions typically limited to Low Earth Orbit (LEO). The AR in the International Space Station (ISS) includes four integrated units, which provide critical functions for life support including Trace Contaminant Control (TCC) system, CO_2 carbon removal branded as Carbon Dioxide Removal Assembly (CDRA), O_2 generation branded as Oxygen Generation Assembly (OGA), and oxygen recovery branded as Carbon Dioxide Reduction System (CDRS).

CDRS is a Sabatier reactor that operates at 300–400 °C and reduces CO_2 to methane (CH_4) and H_2O using H_2 from OGA (an electrolysis unit that generates O_2 as main product and H_2 as byproduct) as reactant. The CDRS limits the feasibility of having a closed loop system, as it requires more water than the water metabolically generated ultimately resulting in a recovery rate of approximately 50%. NASA Marshall Space Flight Center (MSFC) and the University of Texas at Arlington (UTA) are currently developing an Engineering Development Unit (EDU) of a Macrofluidic Electro Chemical Reactor (MFECR) to convert a continuous stream of CO_2 and water into O_2 and C_2H_4 at standard conditions. The novel design combines CO_2 conversion and water electrolysis (currently conducted in OGA and CDRS units respectively) into one compact unit that runs at standard conditions and is theoretically capable of generating O_2 with a theoretical maximum metabolic CO_2 conversion of 73% while consuming less metabolic water. The metabolic CO_2 conversion process that currently operates at the ISS yields CH_4 as waste byproduct losing 4 moles of H (2 moles of H_2 originally generated by 2 moles of water) per 1 mole of C; the novel design yields C_2H_4 as byproduct losing half of the H/ H_2 moles than the current CH_4 -byproduct-producer approach.

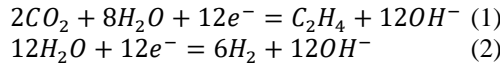
The authors have developed and deployed a comprehensive 3D multiphysics model that thoroughly replicates the actual configuration and fluid/material domains of the MFECR. In the model, the EC physics (multicomponent-multiphase electrochemical-driven reactions leading CO₂ conversion to C₂H₄ and formation of H₂ on the cathode in parallel with formation of O₂ and H₂O on the anode) are coupled with all the other physics phenomena involved in the process including fluid and non-ideal mass transfer of reactant and product species in free and porous media, CO₂ transport from gas phase within porous electrode to liquid phase (electrolyte), condensation/evaporation of water driven by capillary pressure within porous medium, convective/conduction/radiative heat transfer, and conduction of DC electrical current with Joule heating generation.

This model is aimed to conduct quantitative benchmark on three different MFECR geometry layouts having all three the same base surface, one without serpentine paths (plain) and two with serpentines leading to four and twelve paths respectively. Once experimental data is generated via a test matrix of 200 tests, the model will be validated to conduct MFECR process optimization and revalidate the quantitative benchmark on the three different MFECR geometry layouts. The MFECR test stand is fully automated and equipped with several inline measurement (flow, pressure, temperature, pH, component concentration) systems on all six MFECR IO streams allowing reliable experimental validation of the model and parametric determination of all EC reactions. Three key EC reactions are considered in the model, two in the cathode (CO₂-C₂H₄ reduction and H₂ formation) and one on the anode (O₂ formation)

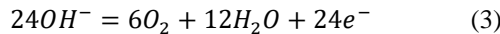
II. Process Fundamentals

A catalysis developed by researchers at University of Texas at Arlington (UTA) selectively reduces CO₂ to C₂H₄ via electrolysis at standard conditions using an alkaline electrolyte, potassium hydroxide (KOH), and yielding H₂ besides C₂H₄ on the cathode and O₂ on the anode¹. These three electrochemical (EC) reactions posted below indicate that hydroxide ions (OH⁻) are generated on the cathode via reduction of CO₂ to C₂H₄ and H₂O to H₂, then transported through the electrolyte to the anode and consumed in the formation of O₂. While all OH⁻ generated on the cathode is consumed on the anode, H₂O consumed on the cathode is not entirely generated on the anode due to the formation of C₂H₄ byproduct yielding a net H₂O consumption (still lower than in the case of CH₄ byproduct generation in Sabatier's approach) as illustrated below.

Cathode:



Anode:



Total:

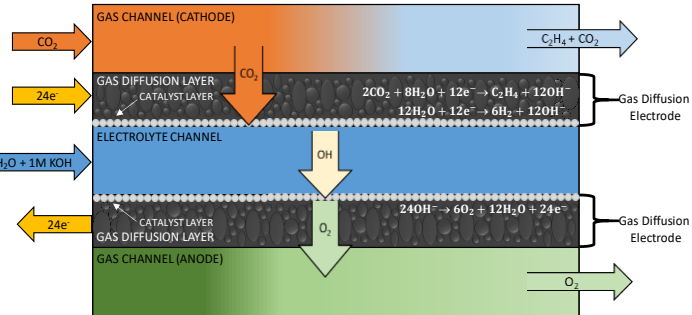
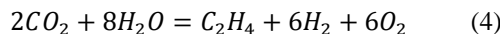


Figure 1. Schematic of EC process in the MFECR.

Figure 1 depicts a schematic of the EC process in the MFECR equipped with three flow streams that carry cathodic CO₂ reactant, KOH electrolyte solution, and anodic O₂ product respectively along with two conducting gas diffusion electrodes (GDE) that have three layers, the gas diffusion layer (GDL), the macropore layer (MP), and the catalysis layer (CL) as illustrated in Figure 2. In the cathode channel CO₂ diffuses through the GDL reaching the MPL that houses the CL formed by electrochemical (EC) deposition of a copper-based catalysis in direct contact with the KOH aqueous-electrolyte flow stream to yield not only the reduction of CO₂ to C₂H₄ (reaction 1) but also the formation of H₂ (reaction 2) from H₂O. CO₂ and H₂ products diffuse back to the cathode channel mixing with unreacted and depleted CO₂ gas stream. In the anode channel, O₂ is generated (reaction 3) at the CL (coated with platinum/nickel and in direct contact with aqueous-electrolyte flow stream) and

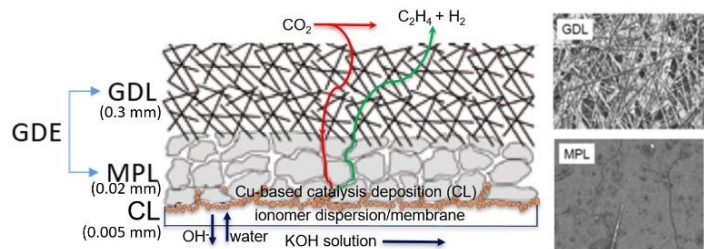


Figure 2. Schematic of GDL, MPL, and CL domains housing the species generated at the CL of the cathode GDE.

diffuses throughout the GDL reaching the anode gas flow stream. As indicated in reaction 4, CO₂ reduction reaction consumes water to yield C₂H₄, H₂ and O₂ leading to an increment in OH⁻ concentration in the electrolyte stream and requiring water makeup to keep the desired OH⁻ concentration in the aqueous electrolyte. Researchers have reported other competing reactions on the cathode yielding different C₁ and C₂ products with copper-based catalysis²; UTA researchers have developed a unique and proprietary copper-based catalysis that selectively yields C₂H₄ over CO and CH₄ contrary to other Cu-based catalysis reported in the literature³. CO and CH₄ are more undesired byproduct than C₂H₄ as the formation of CO reduces O₂ recovery and the formation of CH₄ consumes more water than the formation of C₂H₄ since it has lower H/C ratio, 2 for C₂H₄ and 4 for CH₄. The model neglects these two EC reactions yielding CO and CH₄ byproducts in the cathode as their compositions in the outlet stream using proprietary UTA's catalysis have shown to be lower than 2%.

III. Model Domains

The material domains used in the 3D model are replicas, at EDU scale, of the actual MFECR's material domains; the drawings generated to fabricate the MFECR's domain components were also used as spatial material domains in the 3D model along with the commercially available GDE's domains bearing three subdomains (GDL, MPL, and CL) with spatial dimensions provided by their manufacturers.

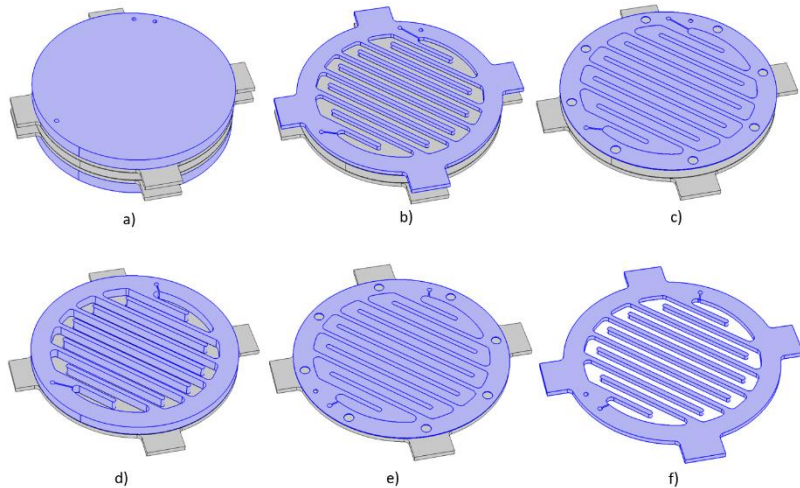


Figure 3. MFECR's model material domains (colored in purple): a) top and bottom endplates, b) cathode serpentine channel, c) cathode GDE (housing GDL, MPL, and CL subdomains), d) electrolyte serpentine channel, e) anode GDE (housing GDL, MPL, and CL subdomains), and f) anode serpentine channel.

The eleven MFECR's material domains include two non-electrical-conducting endplates to press the EDU on the cathode and anode ends respectively, two electrical-conducting serpentine channels to house the CO₂ (cathode) and O₂ (anode) gas flow streams, one non-electrical-conducting electrolyte serpentine channel to house the electrolyte liquid flow stream, and two GDEs (cathode and anode), each one housing three material subdomains that include the gas diffusion layer (GDL), the MPL, and the CL. MPLs are typically built up by a mixture of carbon black powder and a hydrophobic agent, typically poly-tetra-fluoro-ethylene (PTFE). GDL works as a protective layer for the delicate catalyst structure, provides good mechanical strength and easy gas access to the catalyst, and improves the electrical conductivity. MPL reduces the contact resistance between catalyst layer and microporous substrate.

Besides the eleven spatial material domains described above, the model also includes three fluid domains flowing along the cathode, electrolyte, and anode serpentine chambers respectively. These three flow domains were created by generating a solid material domain of the entire MFECR and subtracting all eleven spatial material domains (two endplates, three serpentine channels, two GDLs, two MPLs, and two CLs). Each cathode and anode flow domain has three subdomains to house the cathode and anode streams throughout four different flow media that correspond to one free flow along the serpentine channel and three porous flows along the GDL, MPL, and CL.

Figure 3 depicts the key material domains colored in purple, a) top and bottom endplates, b) cathode serpentine channel, c) cathode GDE (housing GDL, MPL, and CL subdomains), d) electrolyte serpentine channel, e) anode GDE (housing GDL, MPL, and CL subdomains), and f) anode serpentine channel. The materials used in the actual MFECR elements and assigned to the corresponding model's material domains include polycarbonate for the endplates, Teflon for the electrolyte serpentine channel, nickel for the anode and cathode serpentine channels, and porous carbon-based composite for the GDEs. The physical properties of these material domains that include but not limited to density, thermal conductivity, heat capacity, electrical conductivity, and thermal radiative emissivity are set in the model as temperature dependent.

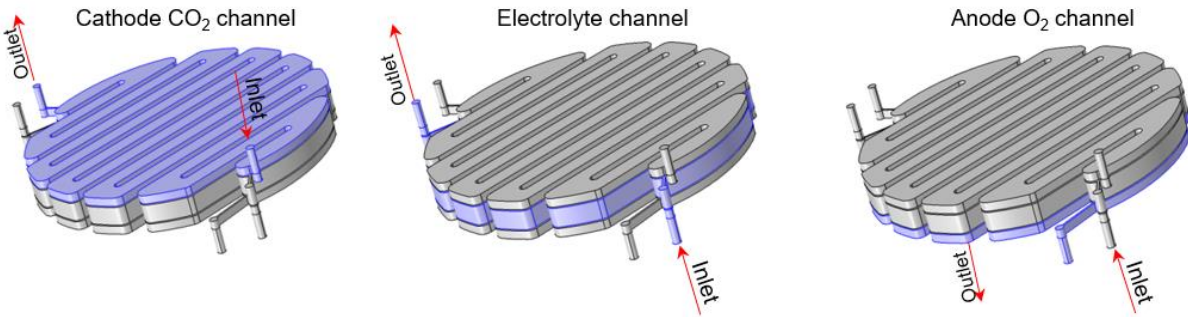


Figure 4. Flow domains and I/O streams for the cathode, electrolyte, and anode serpentine channels.

Figure 4 illustrates the flow domains, and the direction of the IO flow streams in each serpentine channel corresponding to the cathode (CO_2 gas), electrolyte (aqueous KOH solution), and anode (O_2 gas). The physical properties of these flow domains that include but not limited to viscosity, thermal conductivity, electrical conductivity, and diffusion coefficients are also set in the model as temperature dependent.

Model Definition

The EC reaction section of the MFECR consists of two porous CLs and an electrolyte serpentine channel sandwiched in the middle as shown in Figure 5. The CO_2 feeds the cathode serpentine channel and part of the O_2 product is fed back to the anode serpentine chamber. The alkaline solution feeds the electrolyte serpentine chamber wetting the CLs of both, the anode and cathode GDEs allowing the OH^- ionic transport between them. The EC reactions in the cell are reactions (1) and (2) in the cathode's GDE and reaction (3) in the anode's GDE yielding the total reaction (4).

The model includes the following processes:

- Electronic charge balance (Ohm's law)
- Ionic charge balance (Ohm's law)
- Concentration-dependent Butler-Volmer and Tafel charge transfer kinetics
- Flow distribution in gas and liquid channels (Navier-Stokes)
- Flow in the porous GDL, MPL, and CL (Brinkman equations)
- Mass balances in gas phase in both gas channels and porous GDL, MPL, and CL (Maxwell-Stefan diffusion and convection)
- Evaporation and condensation of water on the GDL and gas channels along with condensed water transportation through the GDL's porous via capillary pressure.
- Temperature-pressure dependent CO_2 absorption/dilution into KOH aqueous electrolyte solution via Henry constant.
- Temperature (energy balance equation) via three types of heat transfer mechanisms,
 - 1) conductive within EDU's components,
 - 2) convective within the channel flows,
 - 3) radiative between EDU surface and ambient
- Heat generation/source via Joule heating effect.

A. EC Reaction Phase

Species generated in EC reactions 2) and 3) are assumed to yield gaseous products, H₂ in the cathode (reaction 2), O₂ as well as water vapor in the anode (reaction 3). Temperature-pressure dependent condensation of the water vapor generated at the anode (reaction 3) is estimated as well as its transportation through the porous GDE and MPL domains driven by the porous capillary pressure. In the CO₂ reduction (CO₂R) to C₂H₄ (reaction 1) the CO₂ reactant is still assumed to be in the gas phase but dissolved in the aqueous KOH electrolyte as recent experimental and theoretical work have demonstrated the importance of water and hydrated cations on the elementary processes involved in CO₂R superseding the role of CO₂ gas phase within the GDLs. Therefore, researchers have proposed that it is necessary for the catalyst to be covered with electrolyte to be active. This means that although CO₂ is supplied to the GDE from the gas phase, the reactant at the catalyst site is still dissolved CO₂.

B. Charge Balances

The electronic and ionic charge balance in the cathode and anode current feeders, the electrolyte, and GDEs are solved for using a secondary current distribution interface that accounts for the effect of the electrode kinetics in addition to solution resistance. The model assumes that concentration-dependent Butler-Volmer charge transfer kinetics describes the charge transfer current density for the EC reactions except for CO₂ as the EC reaction is assumed to take place in the gas phase but after diluted into the electrolyte wetting the catalysis. At the cathode, CO₂ is reduced to C₂H₄ and H₂ is concurrently formed as stated in reactions (1) and (2) respectively; assuming the first electron transfer to be the rate-determining step, the following charge-transfer kinetics equations apply for reactions (1) and (2) respectively:

$$i_{c,co_2} = i_{o,co_2} \left(\frac{c_{co_2}}{c_{co_2,ref}} \exp\left(\frac{\alpha_{c,co_2}F}{RT}\eta\right) - \frac{c_{c_2h_4}}{c_{c_2h_4,ref}} \exp\left(\frac{-\alpha_{a,co_2}F}{RT}\eta\right) \right) \quad (5)$$

$$i_{c,h_2} = i_{o,h_2} \left(\frac{c_{h_2}}{c_{h_2,ref}} \exp\left(\frac{\alpha_{c,h_2}F}{RT}\eta\right) - \exp\left(\frac{-\alpha_{a,h_2}F}{RT}\eta\right) \right) \quad (6)$$

Here i_{o,co_2} and i_{o,h_2} are the cathode exchange current densities (A/m²) for the cathode reactions (1) and (2), c_{co_2} , $c_{c_2h_4}$, c_{h_2} are the molar concentrations of CO₂, C₂H₄, and H₂ respectively, $c_{co_2,ref}$ and $c_{c_2h_4,ref}$ are the reference concentrations (mol/m³). α_{c,co_2} , α_{a,co_2} , α_{c,h_2} , α_{a,h_2} are the cathodic/anodic charge transfer coefficients for the cathode reactions (1) and (2) respectively. Furthermore, F is Faraday's constant (C/mol), R the gas constant (J/(mol·K)), T the temperature (K), and η the overpotential (V).

For the anode, the following charge transfer kinetics equation applies for reaction (3)

$$i_{c,o_2} = i_{o,o_2} \left(\frac{c_{o_2}}{c_{o_2,ref}} \exp\left(\frac{\alpha_{c,o_2}F}{RT}\eta\right) - \exp\left(\frac{-\alpha_{a,o_2}F}{RT}\eta\right) \right) \quad (7)$$

Here i_{o,o_2} is the anode exchange current density (A/m²) for the anode reaction (3), c_{o_2} is the molar concentration of O₂, $c_{o_2,ref}$ is the reference concentration (mol/m³). α_{c,o_2} , α_{a,o_2} are the cathodic/anodic charge transfer coefficients. The overpotential η is defined as

$$\eta = \Delta\phi_{electronic} - (\Delta\phi_{ionic} + \Delta\phi_{eq}) \quad (8)$$

Where $\Delta\phi_{eq}$ is the equilibrium potential difference (SI unit: V). The concentration-dependent kinetics expressions (5), (6) and (7) are used to set up the charge transfer expressions that lead to $\Delta\phi_{ionic}$ value.

At the cathode's inlet boundary, the potential is set at a reference potential of zero (ground). At the anode's inlet boundary, the potential is set to the cell potential V_{cell} . The cell polarization V_{pol} is then given by

$$V_{pol} = (\Delta\phi_{eq,c} - \Delta\phi_{eq,a}) - V_{cell} \quad (9)$$

Where $\Delta\phi_{eq,c}$ and $\Delta\phi_{eq,a}$ are the total equilibrium differential potential of all individual species participating in the EC reactions on the cathode and the anode respectively.

C. Multicomponent Transport

At the cathode serpentine channel, CO₂ gas is supplied as reactant, meaning that the gas in the channel and GDE consists of three components: unreacted CO₂ and products C₂H₄, and H₂. In the anode, O₂ product is resupplied, consisting of two product components: O₂ and water vapor. Nitrogen (N₂) is used as a carrier gas for the product O₂ and water vapor.

The material transport is described by the Maxwell-Stefan's diffusion and convection equations, solved by using a transport of concentrated species interface for each electrode flow serpentine channel. The boundary conditions at the walls of the gas channel and GDE are zero mass flux (insulating condition). At the inlet, the composition is specified, while the outlet condition is convective flux. This assumption means that the convective term dominates the transport perpendicular to this boundary. Continuity in composition and flux apply for all mass balances at the interfaces between the GDEs and the serpentine channels.

D. Gas and Liquid Flow Equations

The Brinkman equation describes flow in porous media where momentum transport by shear stresses in the fluid is of importance. The model extends Darcy's law to include a term that accounts for the viscous transport, in the momentum balance, and introduces velocities in the spatial directions as dependent variables. In the model, the Brinkman equations interface is used for solving the velocity field and pressure in both the cathode and anode serpentines channels.

The compressible Navier-Stokes equations govern the flow in the open channel sections and the Brinkman equations in the porous GDEs. Couplings for the density, velocity, pressure and net mass sources and sinks are made to the transport of concentrated species interfaces by using reacting flow multiphysics. The incompressible Navier-Stokes equations govern the liquid flow in the electrolyte serpentine channel.

E. Heat Transfer Equations

A general energy balance equation is implemented in the model to obtain the temperature distribution throughout the MFECR including all solid parts and three flows running through the cathode, anode, and electrolyte serpentine channels. The model considers two heat transfer mechanisms for the heat exchange between the MFECR's surface and the ambient, natural convection and thermal radiation. For natural convection, constant heat transfer coefficients are originally assumed based on values found in the literature and finally determined via experimental validation using modeled and experimentally measured temperature values throughout the MFECR's surface. Thermal radiation emissivity of the MFECR's materials is not found in the literature and used in the model to compute the radiative heat transfer mechanism between MFECR's surface and the ambient.

As an electrical potential is applied between the two GDE's, an electrical current is generated and carried throughout the walls of the cathode, anode, and electrolyte serpentine channels, the model accounts for this source of energy transformed in heat generation via the Joule heating effect equation.

IV. Model Implementation

The 3D model was implemented in COMSOL⁴, a cross-platform finite element analysis, solver and multiphysics simulation software. It allows conventional physics-based user interfaces and coupled systems of partial differential equations (PDEs). COMSOL provides an integrated development environment (IDE) and unified workflow for electrical, mechanical, fluid, acoustics, and chemical applications. The complexity and the number of coupled multiphysics involved in the model lead to demanding significant computational power; a typical run case of the model requires 25-30 GB of RAM.

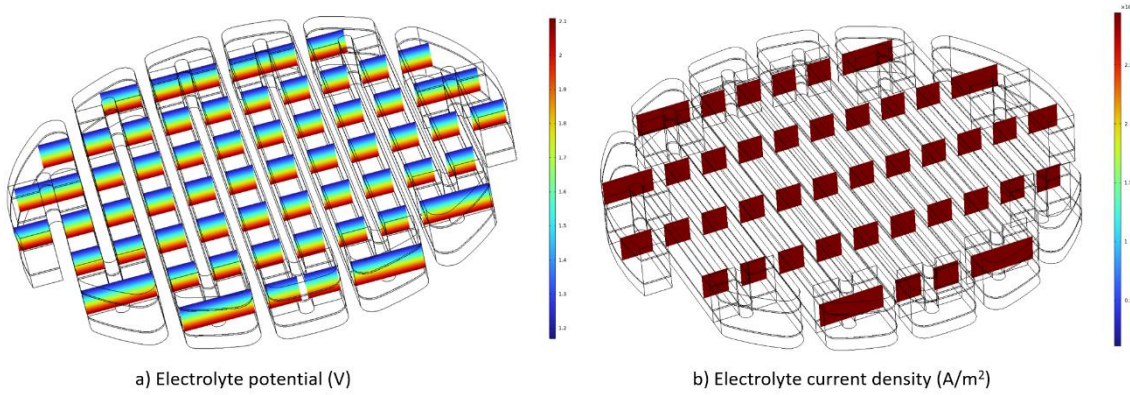


Figure 5. Potential and current density on electrolyte solution as 4 Volts are applied to the MFECR

Figure 5 illustrates the electrolyte potential (4a) and current density (4b) as an electrical potential of 4 Volts is applied on material domains 2b and 2f corresponding to the cathode and the anode serpentine channels respectively. Figure 6a and 6b depict the gas flow profiles (m/s) through the cathode and the anode flow domains illustrated in Figure 4 as 100 sccm of CO_2 and 100 sccm of N_2 are fed to the cathode and anode gas channels respectively; Figures 6c and 6d depict the CO_2 and O_2 weight fractions within the cathode and the anode gas channels depicted 6a and 6b respectively.

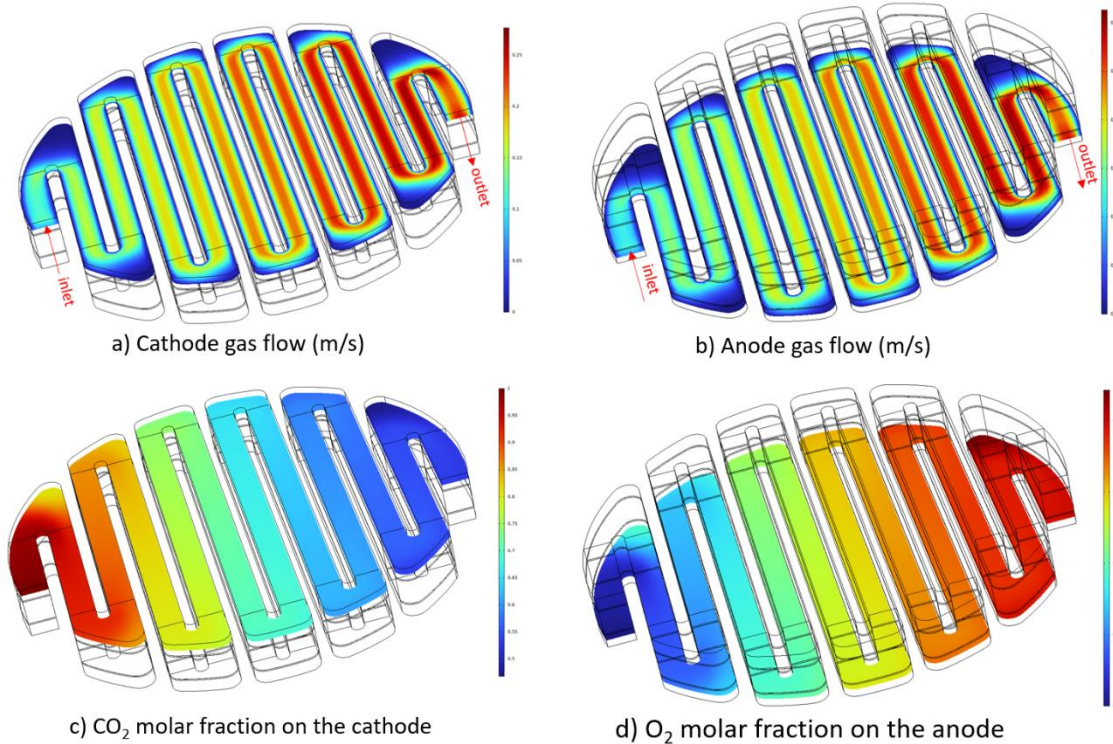


Figure 6. Gas flow profiles through the cathode (a) and the anode (b) serpentine channels as 100 sccm of CO_2 and N_2 are fed to the cathode and anode gas channels respectively; CO_2 (c) and O_2 (d) weight fraction profiles through the cathode and the anode gas channels a) and b) respectively

The Brinkman equation is used for solving the velocity field and pressure in both the cathode and anode serpentines channels as these gas flows have two regimes, free flow in the hollow channel and porous flow in the GDE. The

Navier-Stoke equation with laminar flow assumption is used for solving the velocity field and pressure of the aqueous solution in the electrolyte serpentine channel.

As illustrated in Figure 6, CO₂ depletes at expenses of the C₂H₄ and H₂ generation enriching the cathode gas flow with C₂H₄, and H₂ as the CO₂ and H₂O continue reacting yielding C₂H₄ and H₂ respectively and flowing toward the channel's end.

C₂H₄ and H₂ once are generated on the CL coated with copper-based catalysis, both diffuses through the MPL and GDL to reach the serpentine channel and mix with the flowing CO₂-depleted gas stream. On the anode serpentine-channel side, O₂ is generated on the CL coated with Platinum/Nickel (Pt/Ni) and diffused through the MPL and GDL reaching the carrier (N₂) gas used to feed the anode serpentine channel.

Figure 7 depicts the temperature profile of the a) MFECR's surface and b) electrolyte KOH solution flow that is fed at 277 K having set at an ambient temperature of 300 K. The model considers two sources of heat exchange with the environment (natural convection and thermal radiation) as well as one heat source (Joule heating effect).

The model uses different constant natural convective heat transfer coefficient on three MFECR's surface areas, two (horizontal and vertical) open areas and one horizontal underneath area. The value of each of these three coefficients will be experimentally determined through experimental validation by measuring temperature throughout the MFECR's surface.

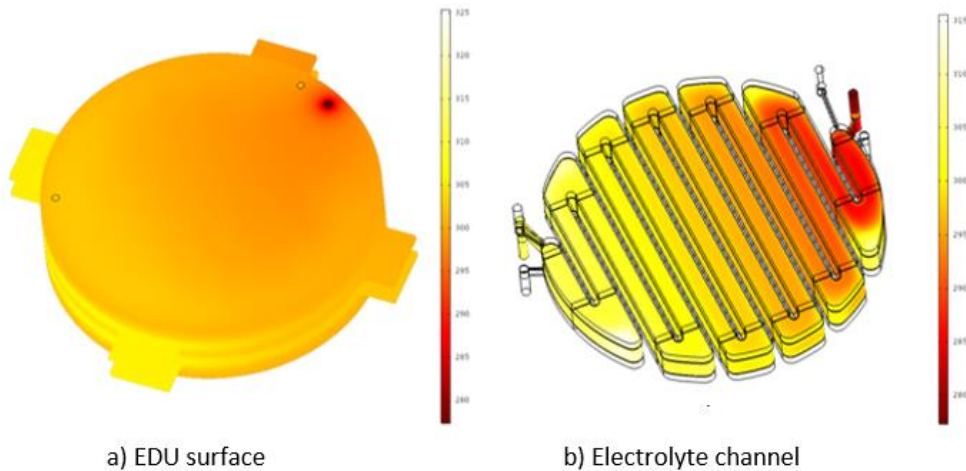


Figure 7. Temperature (K) profile throughout the a) MFECR's surface and b) electrolyte serpentine channel as KOH solution is fed to the electrolyte serpentine channel at 277 K having an ambient temperature of 300 K.

As illustrated in Figure 7a, the cold electrolyte feed stream generates a cold spot on the MFECR's endplate surface. Figure 7b shows that the electrolyte temperature increases as the KOH solution flows toward the electrolyte channel's exit due mainly to heat flux gained from not only the ambient (natural convection and thermal radiation) but also the Joule-heating effect.

As electrical potential is indeed applied on each of the four ears of both (cathode and anode) serpentine channel domains shown in Figures 3b and 3f respectively, the actual differential potential within the EC cell (between the two GDEs) happens to be lower than the electrical potential applied on the ears as the two joint materials (nickel-based channel and carbon-based GDE) have different density and electrical conductivities. The model correctly sets the experimental operating potential value as boundary conditions on the ear's surface. As illustrated in Figure 8, a potential of 2.5 V is applied to each of the four ears of the cathode serpentine channel (dark red region) while ground (0 V) is applied to the anode (dark blue). The modeled

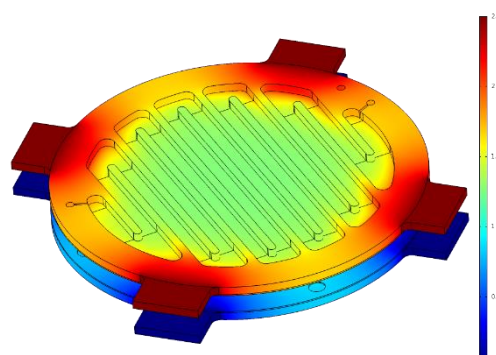


Figure 8. Electrical potential on serpentine channels and GDEs as a potential difference of 2.5 V is applied to the channel's ears.

electrical potential decreases substantially on the GDE surface that is the floor of the serpentine channel, from 2.5 V to 1.6 V (light yellow region) near the body-channel wall and 1.4 V (light green) along the serpentine channel.

V. Model Validation

The model developed and deployed by the authors at MSFC has the multiphysics foundations and rigor to simulate the actual EC process allowing the user to optimize the design and operation of the MFECR aimed and manufactured at EDU scale to efficiently yield metabolic CO₂ reduction to C₂H₄ and generate H₂ and O₂ as byproducts at ambient conditions. The MFECR is installed in a test stand at MSFC equipped with all the instrumentation and sensors that will allow the validation of the model including determination of the EC kinetics parameters for the key EC reactions that take place on the cathode and the anode CL domains.

All inlet-outlet (IO) streams of the MFECR are fully monitored inline yielding and logging data on a) flow rate, temperature, and pressure for all IO streams, b) pH on both input and output KOH solution streams, and c) gas composition on the cathode and anode outlet gas streams. The IO streams include 1) the inlet CO₂ gas and outlet product streams at the cathode serpentine channel, 2) the inlet O₂ carrier gas and the outlet product streams at the anode serpentine channel, and 3) the inlet and outlet KOH-solution streams at the electrolyte serpentine channel.

Assuming electron transfer is the rate-determining step on both GDEs, the concentration-dependent Butler-Volmer charge-transfer kinetics yields three parameters (exchange current density i_o , cathodic charge transfer α_c , and anodic charge transfer α_a) for each one of the three EC reactions considered in the MFECR's model, reactions 1 (CO₂ reduction), 2 (H₂ formation) and 3 (O₂ formation).

VI. Qualitative Benchmark on EDU Configurations

Keeping MFECR's performance requires that the CO₂ flow pattern within the MFECR can access the entire catalyst surface to maximize catalyst utilization and the desired CO₂ reduction to C₂H₄. We used the model to conduct a qualitative benchmark on two flow fields as shown in Figure 9, the flow pattern currently being used in the tests with serpentine bearing 12 paths and one flow pattern without serpentine bearing a single path. The serpentine of the original MFECR's domain was removed to generate the domain for the flow pattern without serpentine; the same operating conditions were used for both flow patterns.

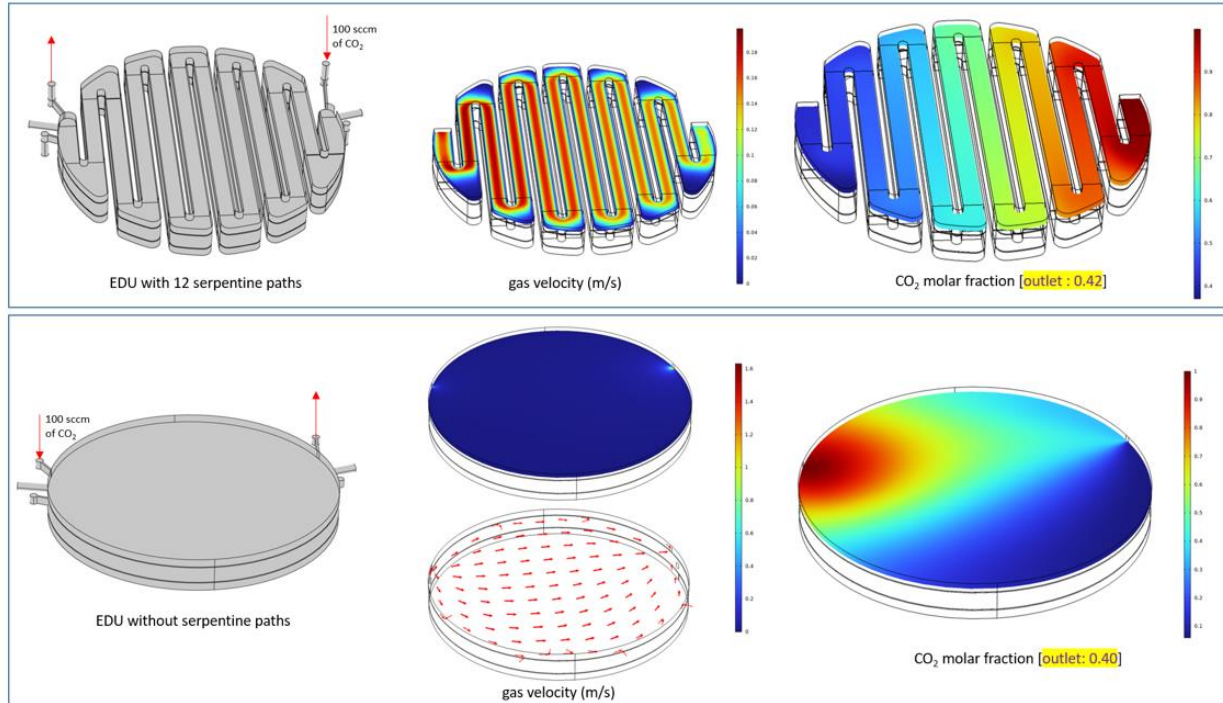


Figure 9. Modeled-based estimation on CO₂ reduction under two flow patterns, one with serpentine bearing 12 paths and the other without serpentine.

The two different flow patterns were modeled to better understand the geometric factors impacting catalyst utilization on the reduction of the CO₂ to C₂H₄. The cathode pressure drop is supposed to play the most critical role in maintaining catalyst utilization at all time scales by encouraging in-plane CO₂ transport throughout the GDL⁵; since the serpentine flow channel has higher pressure drop is then the most failure-resistant. Equally important to take in account is the fact that the serpentine wall compressed the GDE underneath the wall altering its mechanical properties, including the void fraction and the GDL/MPL interface, that might lead to the degradation of not only the GDE underneath the serpentine wall but also the general process outcome.

In the case illustrated in Figure 9, an inlet CO₂ flow of 100 sccm is fed in both MFECRs having different flow patterns, with and without serpentine, yielding similar CO₂ molar concentration on the outlet side, 42% and 40% (highlighted in yellow) for flow patterns with and without serpentine respectively.

References

- ¹ Brown B. R., Curreri P. A., Rabenberg E. M., Dominguez J. A., Reidy L. P., Dennis B., Chanmanee W., Burke K. A., Developmental efforts of an electrochemical oxygen recovery system for advanced life support, International Conference on Environmental Systems (ICES), 50th International Conference on Environmental Systems, paper 74, pp. 11-12.
- ² Y. Hori: Electrochemical CO₂ reduction on metal electrodes. In Modern Aspects of Electrochemistry, Vol. 42, C.G. Vayenas, R.E. White, and M.E. Gamboa-Aldeco, eds. (Springer, New York, 2008); pp. 89-189.
- ³ Tacconia N. R., Chanmanee W., Dennis B., Rajeshwarb K., Composite copper oxide–copper bromide films for the selective electro-reduction of carbon dioxide, J. Mater. Res., Vol. 32, No. 9, May 15, 2017; pp. 1727-1724
- ⁴ COMSOL, Electrochemistry Module User's Guide, Software Manual – User Guide, Version: COMSOL 5.4, 2018. <https://doc.comsol.com/5.4/doc/com.comsol.help.echem/ElectrochemistryModuleUsersGuide.pdf>
- ⁵ Subramanian S., Li M., Yang K., Sassenburg M., Geometric Catalyst Utilization in Zero-Gap CO₂ Electrolyzers, ACS Energy Lett. 2023, 8, 222–229.